The Peruvian upwelling system. A numerical study of the spatial and time variabilities

Enrique Huaringa*[1]

[1] *Consultor*

Abstract

One of the most important upwelling areas is off the Peruvian coast. Two regions are especially prominent: $11°$ to $12°$S and $14°$ to 15oS. The upwelling is most intense in the northern area. In addition to the spatial change, there is a time variation with a pronounced annual period, with the maximum upwelling in the southern hemisphere winter. The Peruvian Current leaving the coast in this region may generate special conditions. A change in the whole system occurs when El Niño takes place. The Equatorial Front advances far to the south and coastal upwelling is suppressed. Compared to the large-scale aspects of the El Niño phenomenon itself, its impacts on the Peruvian upwelling system is much less well known. The work is to apply a numerical model and use the data generated by the observational program for calibration and validation purposes.

Keywords: Peruviant current, upwelling areas, numerical model, El Niño phenomenon.

El sistema de afloramiento Peruano. Un estudio numérico de las variabilidades espaciales y temporales

Resumen

Una de las áreas de surgencia más importantes se encuentra frente a la costa peruana. Dos regiones son especialmente prominentes: $11°$ a $12°$S y $14°$ a $15°$S. La surgencia es más intensa en la zona norte. Además del cambio espacial, hay una variación de tiempo con un período anual pronunciado, con el máximo de surgencia en el invierno del hemisferio sur. La corriente peruana que sale de la costa en esta región puede generar condiciones especiales. Se produce un cambio en todo el sistema cuando se produce El Niño. El Frente Ecuatorial avanza hacia el sur y se suprime el afloramiento costero. En comparación con los aspectos a gran escala del fenómeno de El Niño en sí, sus impactos en el sistema de surgencia peruano son mucho menos conocidos. El trabajo consiste en aplicar un modelo numérico y utilizar los datos generados por el programa de observación para fines de calibración y validación.

Palabras clave: Corriente peruana, Areas de afloramiento, Modelo numérico, El fenómeno del Niño.

Introduction

In the study area, the trade winds blow predominantly parallel to the coast making the upwelling system highly sensitive to variability in the intensity of the wind stress. The rise of coastal sea temperatures due to the weakening of coastal upwelling causes the reduction of important fish stocks and other coastal resources of economical significance, especially the sardine and anchovy populations. Two regions of coastal upwelling are especially prominent: $11°$S to $12°$S, and $14°$S to $15°$S. Along the Peruvian coast ($5°$S to $18°$S), alongshore winds are permanent, with a maximum in winter. Sea surface temperature (SST) signature of the upwelling is ambiguous at those latitudes: it is characterized by a negative zonal gradient, lowest SST at the coast (Carr et al., 2002). The most consistent and strongest upwelling center on the Peruvian coast occurs near San Juan at $15°$S, which is representative of onshore-offshore Ekman transport and Ekman pumping during 1996-1997 La Niña event and

---

*enrique.huaringa@gmail.com

1997-1998 strong El Niño event. In the south east Pacific, pumping effect has been locally investigated by Halpern (2002), he suggests that strong negative Ekman pumping may be the source of the deepened coastal thermocline at

15°S during 1997-1998 strong El Niño event. We are tuning the Princeton Ocean Model (Blumberg and Mellor, 1987) that has been designed to represent ocean physical (Ekman dynamic) as realistically as possible.
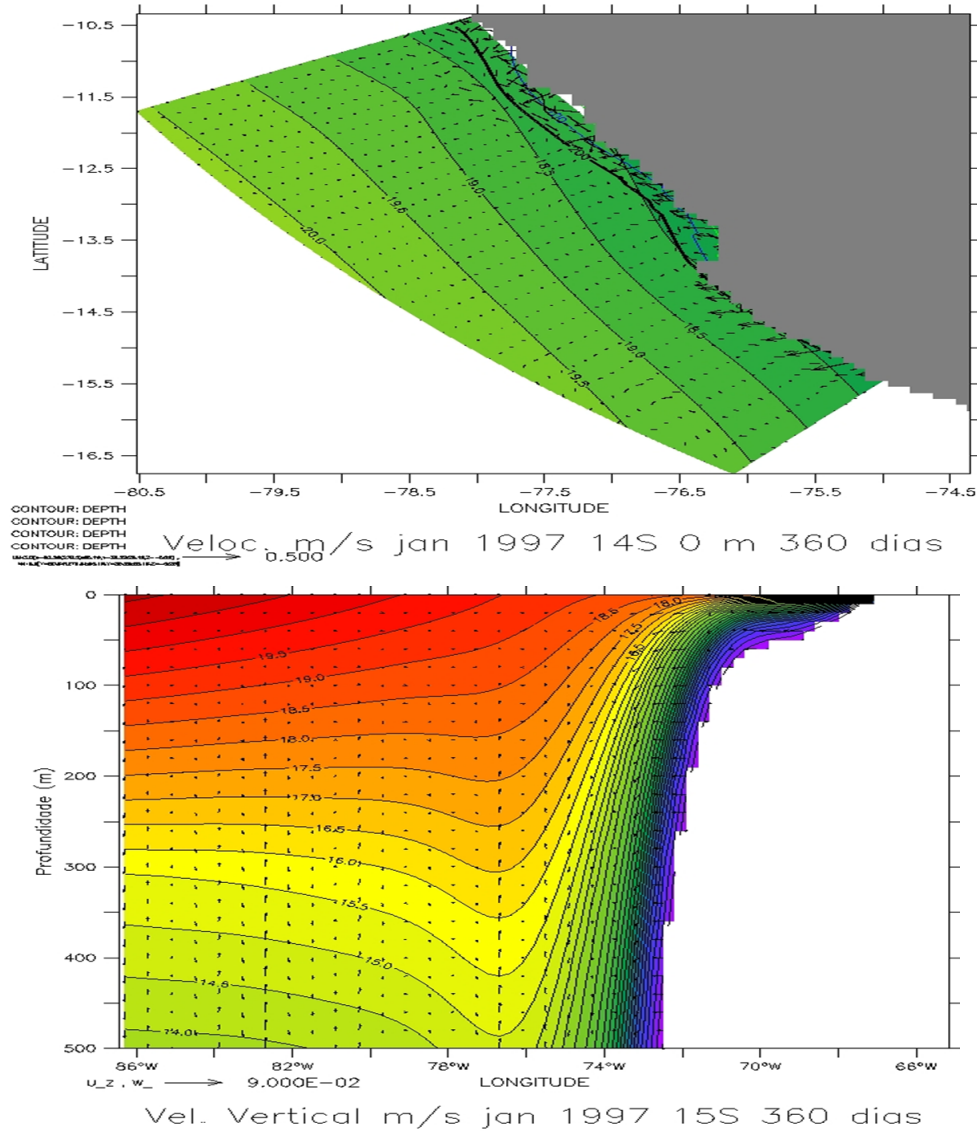

Figure 1: Sea surface velocity (m/s $\times 10^{-2}$) at 14°S January 1997 and upward vertical velocity (m/s $\times$ 10-4) 0-500 m depth at 15°S January 1997

1   Methodology

The Princeton Ocean Model (POM) is a three-dimensional baroclinic nonlinear hydrodynamic model. I generate curviline grids of area of study using a package called gridpak(Wilkin, 1998). The heart of this package is a program which creates an orthogonal grid when

provided with the boundary information. The other programs aid in the defining of the grid boundary and finding the bathymetry (Earth Topography at 5 min resolution ETOPO5) on the finished grid. I have compiled climatologic data of wind stress (IFREMER-CERSAT, 2000), data of temperature (Levitus and Boyer, 1994a) and data of salinity (Levitus and Boyer, 1994b) clima-

tology with spatial resolution of 1° and interpolated for each 2 min. The model uses a sigma coordinate system, where the horizontal x and y coordinates of the traditional Cartesian coordinate system, remain unchanged and the z coordinate is converted to the sigma coordinate, which is scaled according to the depth of the water column. I compute the Ekman pumping using the equation (1), where τ and τ_x are surface wind stress and

its east-west component, respectively, and β is the latitudinal variation of the Coriolis parameter. I realize a preliminary experiment to tune the model, with these results we study the oceanic circulation and Ekman dynamic along the Peruvian coast when occur the El Niño and La Niña events.

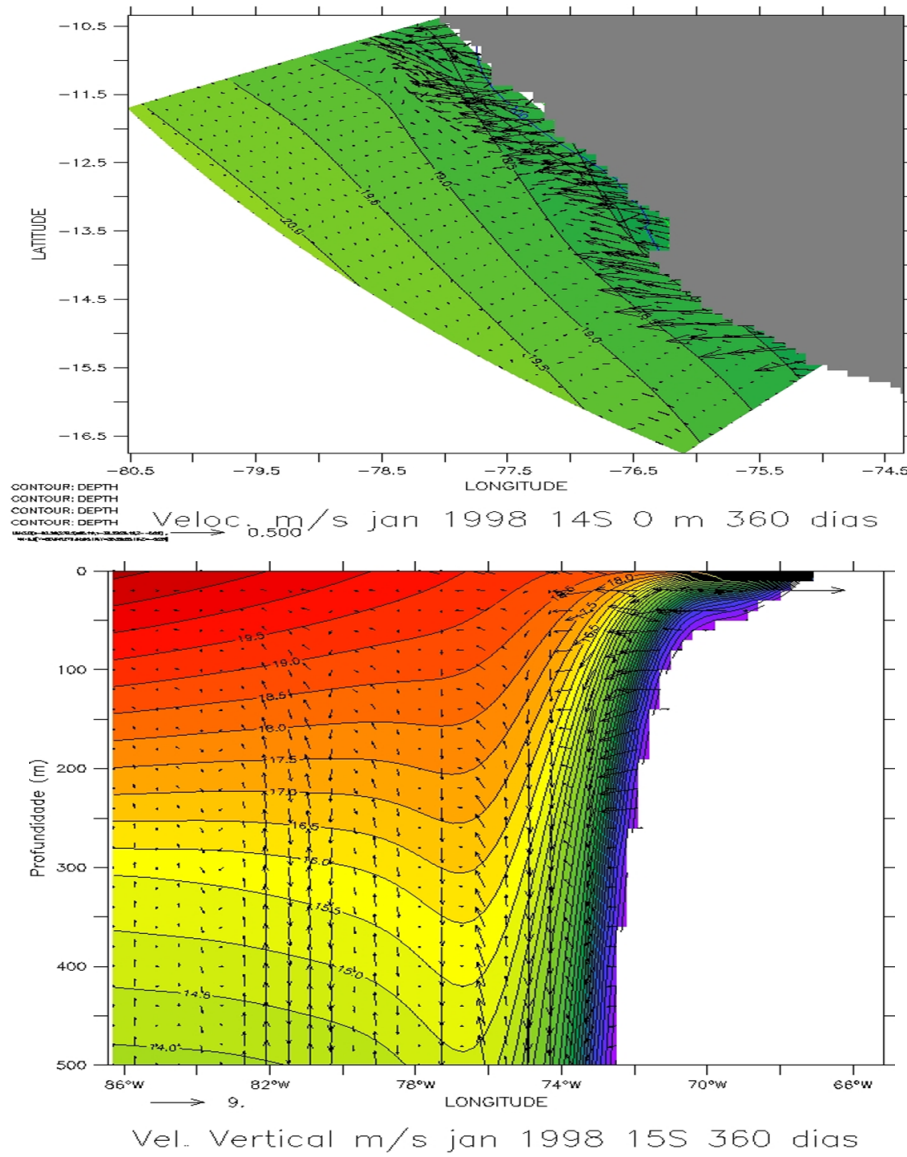$$W_{EK} = \frac{\nabla \times \tau}{\rho f} + \frac{\beta \tau_x}{\rho f^2} \tag{1}$$

Figure 2: Sea surface velocity (m/s $\times 10^{-2}$)) at 14°S January 1998 and upward vertical velocity (m/s $\times 10^{-4}$)), 0-500 m depth at 15°S January 1998.

2   Results

A clear relation between the wind stress and the sea surface temperature (SST) was observed. A complex interaction between offshore Ekman transport, onshore compensation flow, mixed layer depth, and heat gain lead, even with a changing SST, to a persistent offshore SST gradient. The coastal upwelling at 15°S was sustained throughout January 1997 (La Niña event) by alongshore wind stress and Ekman suction because only the crossshore component of the wind stress was reduced. The sea surface velocity (m/s ×10-2) and upward vertical velocity (m/s × 10-4) 0-500 m depth (Figure 1) at 15°S was 4,0 cm/s, low temperatures (18,0 to 20,0°C), strong wind and intense coastal upwelling.

3   Discussion

Our analysis of Ekman pumping/suction at 15°S showed a strong Ekman pumping during July 1996 to March 1997 (La Niña event) was from -40 to -200 and during July 1997 to May 1998 (Strong El Niño event) was from -220 to -230 a similar Ekman pumping. The Ekman pumping have caused the moderate increase in the depth of the coastal thermocline between January 1997 to July 1998, have varied between -40 to -230. The upwelling index provides an estimate of the offshore Ekman transport is computed from the large scale barometric pressure distributions. The sign of the offshore component of the Ekman transport, is then reversed to reflect that negative (offshore) Ekman transport leads to positive (upwelling) vertical transport, and positive (onshore) Ekman transport leads to negative (downwelling) vertical transport (see Figure 3) (Bakun, 1973). The magnitude offshore

Ekman transport component is considered to be an index of the amount of water upwelled from the base of the Ekman layer. Positive values are, in general, the result of equatorward wind stress. Negative values imply downwelling, the onshore advection of surface waters accompanied by a downward displacement of water (Schwing et al., 1996).

In Figure 4, in winter 1997 alongshore wind stress was favourable to upwelling formation via Ekman transport and wind stress intensity increasing offshore creates a positive wind stress curl (Bakun and Nelson, 1991). On the contrary, Ekman transport and wind stress intensity decreasing offshore creates a negative wind stress curl.

Smith (1981) reviewed observations from coastal upwelling studies off Oregon, Peru, and northwest Africa. In all three regions, he found that the offshore, surface layer flow correlated well with the across-shore Ekman transport, he concluded that mass balance was influenced by alongshelf bathymetric variations. The Ekman (or wind drift) layer was less than 25 m thick and in a direction nearly opposite to the flow beneath. Most of the biological productivity occurred within the wind-drift layer and hence tended to move upstream above the upwelling source water, possibly providing a mechanism for seeding and conditioning the upwelling water (Smith et al., 1971). I compared the intensity of Ekman pumping/suction, period 1997-1998, In the Table 1, we observed that speed of Ekman pumping was nearly six (6) times larger than the normal speed of Ekman suction and offshore Ekman transport nearly doubled at 15°S and speed of Ekman pumping was nearly three (3) times larger than the normal speed of Ekman suction and offshore Ekman transport nearly doubled at 5°S.
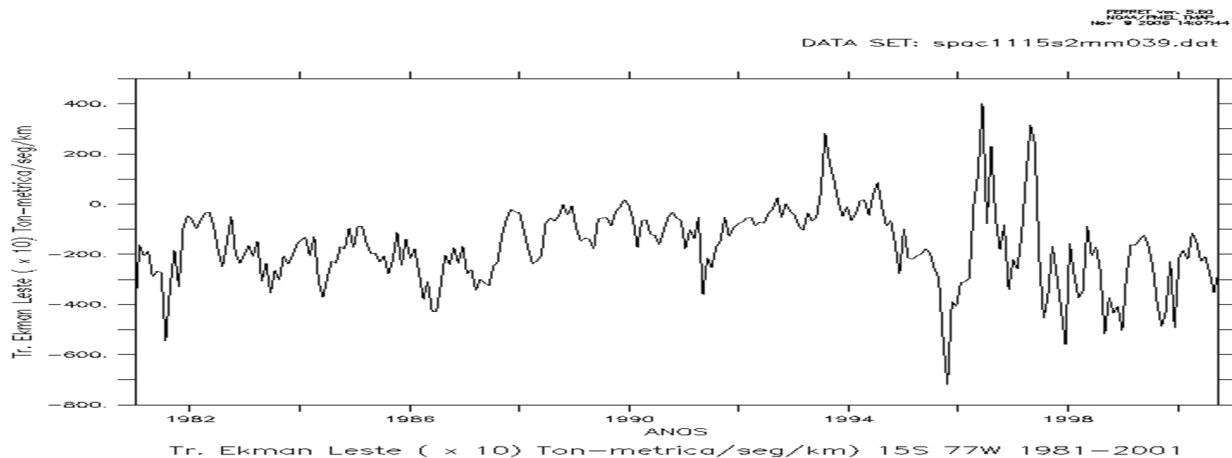

Figure 3: Offshore Ekman transport (metric-tons/sec/100-m coast) 1981-2005 (PFEL, 2005).

Event 1997/1998	Pumping Ekman m^2/s $\times 10^{-6}$ 5°S	ET m^2/s $\times 10^{-6}$ 5°S	Pumping Ekman m^2/s $\times 10^{-6}$ 15°S	ET m^2/s $\times 10^{-6}$ 15°S
Weak La Niña	75	1.497	-35	1.273
El Niño	-25	2.821	-220	2.719

Table 1: Comparation between Ekman transport and Ekman pumping at 5°S and 15°S for January 1997 and January 1998.

4 Conclusions

The numerical simulations were forced with wind products for the 1991-2000 period. These simulations reproduced satisfactorily the average circulation patterns in the study region, confirming that in the areas close to the coast, wind is the main generating mechanism of resurgence or subsidence.

The results showed that during the occurrence of the strong El Niño event from July 1997 to May 1998, in the 15°S radials, there was a drastic change in the coastal resurgence system in response to wind variations.

Both offshore Ekman transport and Ekman suction provided upward velocity during normal oceanographic conditions. However, each mode exhibited different behavior during the July 1997 to May 1998 strong El Niño event when offshore Ekman transport increased compared to normal while normal mild Ekman suction was replaced with intense Ekman pumping.

In the south east Pacific, strong negative Ekman pumping was the source of the deepened coastal thermocline at 15°S during July 1997 to May 1998 strong El Niño event.

By using the equation of continuity the vertical velocity can be estimated from the horizontal current velocities or inferred from the wind (Ekman transport and Ekman pumping), the simulations are reproduced satisfactorily.
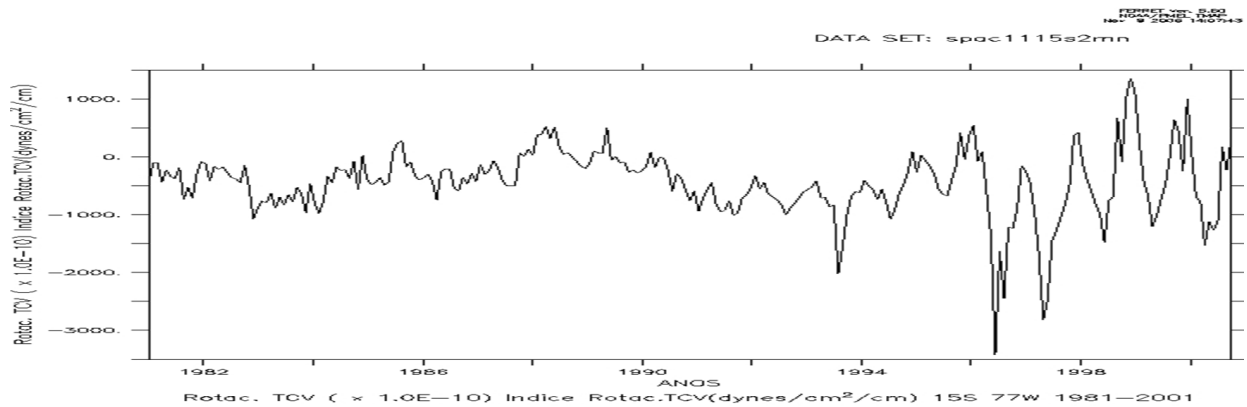

Figure 4: Wind stress curl (dynes/cm2/cm) 1981-2005 (PFEL, 2005).

References

[Bak73] Bakun, A. (1973). Coastal upwelling indices, west coast of north America, 1946-71. U.S. Dep. Commer., NOAA Tech. Rep., NMFS SSRF-671, 103p.

[Bak91] Bakun, A. and Nelson, C. (1991). The seasonal cycle of wind-stress curl in subtropical eastern boundary current regions. J. Phys. Oceanogr., vol. 21, pp 1815-1834.

[Blu87] Blumberg, A. and Mellor, G. (1987). A description of a three-dimensional coastal ocean circulation model. In: HEAPS, N (ed). Three-Dimensional Coastal Ocean Models, Washington: Amer. Geophys. Union, vol. 4, 208p.

[Car02] Carr, M., Strub, P., Thomas, C. and Blanco, J. (2002). Evolution of 1996-1999 La Niña and El Niño conditions off the western coast South America: A remote sensing perspective. J. Geophys. Res., 107, 29,1-29,15.

[Enf81] Enfield, D. (1981). Thermally driven wind variability in the planetary boundary layer above Lima, Peru. J. Geophys. Res., 86, 2005-2016.

[Hal02] Halpern, D. (2002). Offshore Ekman transport and Ekman pumping off Peru during the 1997-1998 El Niño. Geophys. Res. Lett., vol. 2, No. 9, 5, p. 19-1-19-4.

[Huy87] Huyer, A., Smith, R. and Paluszkiewicz. (1987). Coastal upwelling off Peru during normal and El Niño times, 1981-1984. J. Geophys. Res., vol 92, pp 14297-14307.

[IFR02] IFREMER-CERSAT. (2002). Mean wind fields, ERS-1, ERS-2 & NSCAT. C2-MUT-W-05-IF, vol. 1, 52p.

[PFE05] PFEL. (2005). Monthly Mean Upwelling Indices, NOAA, Environmental Research Division, 1981-2005 period.

[Lev94a] Levitus, S. and Boyer, T. (1994a). World Ocean Atlas 1994. National Oceanographic Data Center, Temperature NOAA Atlas NESDIS 3 Dept. of Commerce Ocean Climate Laboratory, v. 1, 117p.

[Lev94b] Levitus, S. and Boyer, T. (1994b). World Ocean Atlas 1994. National Oceanographic Data Center, Salinity NOAA Atlas NESDIS 3, Dept. of Commerce Ocean Climate Laboratory, v. 1, 99p.

[Sch96] Schwing, F., O'Farrell, M., Steger, J. and Baltz, K. (1996). Coastal upwelling indices west coast of North America 1946-1995. NOAA Technical Memorandum NMFS, NOAA-TM-NFMS-SWFSC-231, p. 1-32.

[Smi71] Smith, R., Enfield, D., Hopkins, T. and Pillsbury, D. (1971). The circulation in an upwelling ecosystem: the Pisco cruise. INVESTIGACION PESQUERA, v. 35(1), p. 9-24.

[Smi81] Smith, R. (1981). A comparison of the structure and variability of the flow field in three coastal upwelling regions: Oregon, northwest Africa, and Peru. In: Richards, F. A. (ed.). Coastal Upwelling, Washington: Amer. Geophys. Union, p. 107-118.

[Wil98] Wilkin, J. and Hedström, K. (1998). User's manual for an orthogonal curvilinear gridgeneration package. Technical report.